

## Sidebranch Selection in Fractal Growth

This content has been downloaded from IOPscience. Please scroll down to see the full text.

1991 Europhys. Lett. 16 47

(<http://iopscience.iop.org/0295-5075/16/1/009>)

View [the table of contents for this issue](#), or go to the [journal homepage](#) for more

Download details:

IP Address: 131.111.184.3

This content was downloaded on 26/04/2016 at 12:58

Please note that [terms and conditions apply](#).

## Sidebranch Selection in Fractal Growth.

R. C. BALL, P. W. BARKER and R. BLUMENFELD

*Theory of Condensed Matter, Cavendish Laboratory  
Madingley Road, Cambridge CB3 0HE, UK*

(received 20 March 1991; accepted in final form 17 June 1991)

PACS. 61.50C – Physics of crystal growth.

**Abstract.** – We present a self-consistent theory for the self-similar dendritic structure of noise-reduced diffusion-limited aggregates. We address the sparsening of sidebranches and the mechanism for their ultimate selection in the asymptotic structure. Key predictions are the sidebranch spacing and envelope angle of the dendrite depend crucially on the underlying order of anisotropy.

There are a rich variety of fractal structures produced by irreversible diffusive controlled growth processes [1]. For a fractal structure to be grown by the advance of its perimeter there are two fundamental requirements. To generate ramification of the structure the growth must exhibit frequent tip splitting and/or sidebranching at the smallest scale. To enforce self-similarity there must be competition between branches on all larger scales, so that only of order one branch grows to scale  $R$  in each occupied region of that size.

In this letter we present what we believe to be the first case of an explicit and quantitative theory of how this occurs and of the self-similar structure which results. We focus on noise-reduced diffusion-limited aggregation (DLA) [2-4] with anisotropy, where simulations, see fig. 1, indicate a striking angular morphology and a well-defined hierarchy of scales of sidebranching. The orderliness of this case enabled Eckmann *et al.* [5] to develop an explicit theory of the envelope shape of the major arms, but the underlying fractal structure was not addressed in their work.

Diffusion-controlled growth produces structures where interior fjords are highly screened from the exterior diffusion field. This indicates that the properties and evolution of the growth are mostly governed by the outer envelope of the growth. A successful model for determining the growth singularities of the tips,  $\alpha$ , is to approximate the outer envelope of the tip as a wedge [6, 7]. We use this picture to model the growing dendrite and its sidebranches. The tips of the sidebranches are taken as wedges, enclosed by an imaginary wedge-shaped envelope of head angle,  $\theta_G$  (see fig. 2). The sides of adjacent sidebranch wedges are continued until they meet, to form the simplest realisation of the fjord structure [8]. The growth direction of the sidebranches is fixed by the «angle of attack»  $\phi$ , relative to the main finger. We exploit the orderliness of the growths to model them with an exact self-similar structure. The tips of the upper sidebranches are placed at  $z = x + iy = \lambda^n \exp[i\theta_G]$  and the lower ones at  $z = \lambda^n \exp[-i\theta_G]$ , where  $\lambda (< 1)$  is the geometrical spacing of the sidebranches.

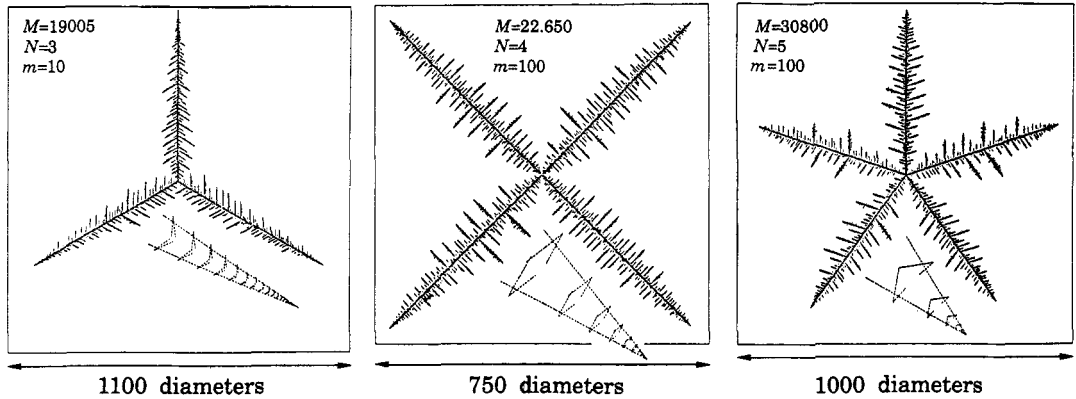


Fig. 1. – High noise-reduced anisotropic DLA clusters of ref. [5]. Each particle has  $n = 3, 4, 5$  «antennas» with equal angles between them. In all cases an asymptotic self-similar structure is approached, with fractal dimension  $D$  between 1.5 and 1.6. (Insets: constructions of the predicted asymptotic sidebranch structure from the theoretical results of table I. The effective wedge angle  $\theta_{\text{eff}}$  is also shown (dashed line).)

We impose the condition that the major sidebranch structure, selected by the competition for growth, is marginally stable [9]. Values can then be calculated for the geometrical spacing of the sidebranches, the envelope angle of their tips, the strength of the leading growth rate singularities (and hence the fractal dimension).

Consider a small corrugation on the selected sidebranches, in which they are alternatively slightly ahead or behind their mean growth rate. If a branch of length  $l$  increases by  $\Delta l$  it is less screened from the diffusion field and its growth velocity  $v$  will also increase. The opposite occurs for branches that are reduced in length. A linear stability analysis shows that marginal stability corresponds to

$$\Delta l/l = \Delta v/v, \quad (1)$$

where  $\Delta v$  is the change in growth velocity. We proceed by considering an alternating corrugation on the sidebranches and use condition (1) to select  $\lambda$  in terms of  $\phi$  and  $\theta_G$ . Only an alternating mode is considered since, by the Mullins-Sekerka instability analysis [10], the shortest wavelength corrugation is the most unstable, and will be the one seen. Consider the conformal map  $z' = z + g(z)$ , where

$$g(z) = z \exp[-i\theta_G] \exp[i\phi] z^{-iv} + z \exp[i\theta_G] \exp[-i\phi] z^{iv}, \quad (2)$$

where  $v = \pi/|\ln \lambda|$ .

The perturbation  $g(z)$  is constructed such that the lengths of the sidebranches are alternatively increased and reduced along their direction of growth. For a sidebranch tip at  $z = \lambda^n \exp[i\theta_G]$ , fig. 2, we obtain  $g(z) = (-\lambda)^n \exp[v\theta_G] \exp[i\phi] + (-\lambda)^n \exp[2i\theta_G] \exp[-i\phi] \cdot \exp[-v\theta_G]$ . The ratio of magnitudes of the second to the first term in  $g(z)$  is  $\exp[-2v\theta_G] \sim 10^{-9}$  (using our results below), and similarly for the first to the second when  $z \propto \exp[-i\theta_G]$  (corrugations on the lower side). Hence, the coupling between corrugations on either side is very weak and that on the upper (lower) side of the wedge can be very well approximated by the first (second) term in  $g(z)$ . So for a sidebranch tip at  $z = \lambda^n \exp[i\theta_G]$ , we take  $g(z) = (-\lambda)^n \exp[v\theta_G] \exp[i\phi]$ . The fractional change of the length of the sidebranch along

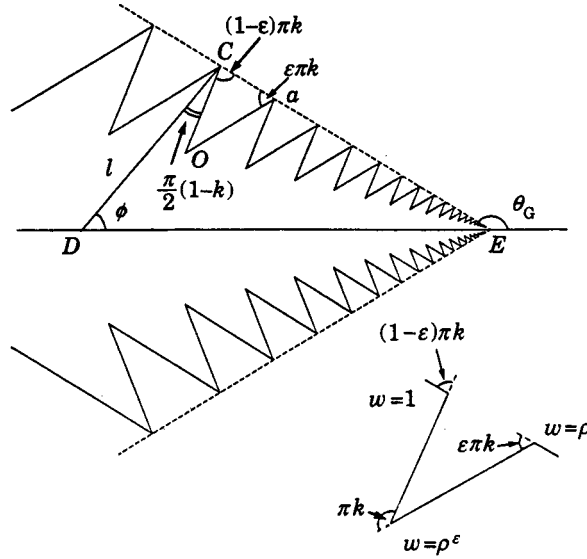


Fig. 2. – The sidebranches of the dendrite are modelled by a self-similar «sawtooth» structure. The anisotropy forces the growth direction of sidebranches to the horizontal to be fixed by the angle  $\phi$ . The dashed line is an imaginary solid cone of head angle  $\theta_G$  enclosing the whole structure. (Inset: the geometrical interpretation of the factor  $(w-1)^{(1-\epsilon)k}(w-\rho)^{\epsilon k}/(w-\rho^\epsilon)^k$  in the Schwarz-Christoffel transformation. Similar basic units, suitably scaled by powers of  $\lambda$ , are connected to give the «sawtooth» structure.) From the triangle  $CDE$ ,  $\phi$  is related to  $\epsilon$  by  $\phi = \theta_G - (1-\epsilon)k\pi - (1-k)\pi/2$ , where  $(1-k)\pi/2 = \pi - \theta_{eff}$ .

its direction of growth is therefore

$$\Delta l/l = (-)^n \exp [v\theta_G] \sin \phi / \sin \theta_G, \tag{3}$$

where  $\lambda^n = l \sin \phi / \sin \theta_G$  has been used. In order to find an expression for the fractional change in the growth velocity we view the dendrite as an isolated charged conductor [11]. The growth velocity is related to the charge within a distance  $r$  of the tip as<sup>(1)</sup>

$$v = (q(r)/r^\alpha)^\eta, \tag{4}$$

where  $\alpha$  is the tip charge singularity and  $\eta$  is the exponent introduced in the dielectric breakdown model [12]. Hence, for any sidebranch tip the new growth velocity,  $v'$  in  $z'$ , is related to the velocity  $v$ , in  $z$ , by

$$v'/q'^\eta = (r')^{-\alpha\eta} = (r|dz'/dz|_{tip})^{-\alpha\eta} = (v/q^\eta)|dz'/dz|_{tip}^{-\alpha\eta}. \tag{5}$$

Under the conformal mapping, tip charges are preserved such that the charge on a tip of radius  $r$  in  $z$  is equal to the charge on a tip of radius  $r'$  in  $z'$ ,  $q'(r') = q(r)$ . This results in

$$v'/v = |dz'/dz|_{tip}^{-\alpha\eta} \approx |1 + (dg(z)/dz)|_{tip}^{-\alpha\eta}$$

<sup>(1)</sup> Note that this form has been constructed so as to give  $v$  independent of the assumed tip radius  $r$ .

and so to first order in  $g$  at the tips of the upper sidebranches,

$$\Delta v/v = -\alpha\gamma \operatorname{Re}(dg(z)/dz) = (-1)^{n+1}\alpha\gamma \exp[\nu\theta_G] \sqrt{1+\nu^2} \cos(\phi - \theta_G - \operatorname{tg}^{-1}\nu). \quad (6)$$

Consequently, condition (1) selects  $\lambda$  in terms of  $\phi$ ,  $\theta_G$  and  $\alpha$  by

$$\sin\phi/\sin\theta_G + \alpha\gamma \sqrt{1+\nu^2} \cos(\phi - \theta_G - \operatorname{tg}^{-1}\nu) \stackrel{!}{=} 0. \quad (7)$$

The growth is self-consistent when the envelope moves as a «bow wave» with  $\lambda$ ,  $\theta_G$  and  $\alpha$  fixed for a given value of  $\phi$ . The velocity of a sidebranch  $v_{sb}$  is related to the main branch velocity  $v_b$  simply by

$$v_b \sin\theta_G = v_{sb} \sin(\theta_G - \phi). \quad (8)$$

The ratio  $v_{sb}/v_b$  can be calculated from the geometry using a Schwarz-Christoffel transformation [13]. For the velocity ratio to be finite, the tip charge singularity of the sidebranches must match the tip charge singularity  $\alpha$  of the main branch. If the wedge were solid, then  $\alpha = \pi/2\theta_G$ , but the ramification of the side structure reduces  $\alpha$  (see below). This defines a new effective cone angle,  $\theta_{\text{eff}} > \theta_G$ , leading to a natural correction to the wedge model. To the best of our knowledge it is the first consistent calculation that gives such a correction.

The conformal Schwarz-Christoffel transformation is used to map the exterior of a polygon in  $z$  onto the upper half-plane in  $w$ , the boundary of the polygon being mapped to the real  $w$  axis. The transformation is written as

$$\frac{dz}{dw} = \prod_{\text{vertices } i} (w - w_i)^{k_i}, \quad (9)$$

where  $k_i\pi$  is the exterior angle turned through (in anticlockwise direction) at each vertex of the polygon.

For the model dendrite of fig. 2 the mapping becomes explicitly

$$\frac{dz}{dw} \propto w^{(1-\alpha)/\alpha} \prod_{n=-\infty}^{\infty} \left( \frac{(w^2 - \rho^{2n})^{1-\epsilon} (w^2 - \rho^{2n+2})^\epsilon}{(w^2 - \rho^{2n+2\epsilon})} \right)^k, \quad (10)$$

where the form of the double infinite product has been severely restricted by the necessary condition that it converge. The main tip is mapped onto  $w = 0$ , the tips of the sidebranches to  $w = \pm \rho^n$  and the fjord vertices to  $w = \pm \rho^\epsilon \rho^n$ . The parameter  $\epsilon$  ( $0 < \epsilon < 1$ ) thus fixes the fjord vertices, but it also gives the factors in (10) the geometrical interpretation shown in the inset to fig. 2. Thus  $\phi$  is given by

$$\phi = \epsilon k\pi + \theta_G - (1+k)\pi/2. \quad (11)$$

The scaling around the main tip can be related to the sidebranch spacing. For the sidebranch tips at  $w = \pm \rho^n$  to correspond to  $z = \lambda^n \exp[\pm i\theta_G]$  we require the mapping  $z(w)$  to have the scaling symmetry  $z(w\rho) = \lambda z(w)$ . Since the infinite product is invariant under  $w \rightarrow \rho w$ , we have  $\rho = \lambda^\alpha$  on comparing with (10), and  $w \propto z^\alpha$  for the scaling around the main tip. The general solution of the scaling equation is

$$w(z) = z^{\ln\rho/\ln\lambda} (A + f_{\text{periodic}}(\ln z/\ln\lambda)),$$

where  $f_{\text{periodic}}$  has period 1 and in all our calculations has amplitude less than  $10^{-3}$  of the constant term  $A$ , along the direction forward from the main tip. We therefore identify the first term with the scaling behaviour around the main tip and it is convenient to represent its exponent in terms of the equivalent effective angle of a conical absorber, giving  $\theta_{\text{eff}} = \pi \ln \lambda / 2 \ln \rho$ . In what follows we also impose the constraint that the scaling around the main tip,  $dz/dw \propto w^{(1-\alpha)/\alpha}$ , matches that around each of the subtips so that  $k = (1-\alpha)/\alpha$ .

The final piece of geometrical information hidden in (10) is the true geometrical angle of the sidebranch tips which can be found (see fig. 2) through

$$\frac{|z_c - z_0|}{|z_a - z_0|} = \frac{\sin(\varepsilon\pi k)}{\sin((1-\varepsilon)\pi k)} = \frac{\sin(\theta_G - \theta_{\text{eff}} - \phi)}{\sin(\theta_G + \theta_{\text{eff}} - \phi)} = \frac{I(\rho^\varepsilon, 1)}{I(\rho, \rho^\varepsilon)},$$

where the last form comes from integrating the SC transformation and

$$I(x_1, x_2) = \left| \int_{x_1}^{x_2} dw w^{(1-\alpha)/\alpha} \prod_{-\infty}^{\infty} ((w^2 - \rho^{2n})^{1-\varepsilon} (w^2 - \rho^{2n+2})^\varepsilon / (w^2 - \rho^{2\varepsilon} \rho^{2n}))^{(1-\alpha)/\alpha} \right|.$$

Given the mapping (10) and its geometrical interpretation we can now compute the crucial ratio of main and sidebranch velocities. In the neighbourhood of vertex  $j$  we identify the singular behaviour of (10) in the form  $dz/dw = A_j(w - w_j)^{(1-\alpha)/\alpha}$ , which upon integration and substitution into (4) yields the tip velocity as

$$v_j = (\alpha A_j)^{-\alpha n}. \quad (12)$$

To summarise our results, we have modelled the structure of the self-similar dendrite in terms of three parameters  $\lambda$ ,  $\theta_G$  and  $\phi$ , and have proposed two equations governing its evolution: eq. (7) (a result of hypothesising that the selected structure is marginally stable) and eq. (8) (the consistency of growth condition). The ratio  $v_b/v_{\text{sb}}$  needed in (8) is calculated from (12). So after fixing one of the physical parameters  $\lambda$ ,  $\theta_G$  or  $\phi$ , the equations may be solved for the remaining two.

A test for the theory is to compare our results against computer simulations performed by Meakin [5]. In the simulations highly «noise reduced» diffusion-limited aggregates ( $\gamma = 1$ ) were grown, in which the local growth anisotropy (and hence the angle of attack of the sidebranches) was fixed. In table I, we compare our analytic results for  $\lambda$  and  $\theta_G$ , with that simulation for different values of their fixed parameter  $\phi$ .

The predicted geometrical angles agree well with simulation, but we found difficulty in measuring an absolute  $\lambda$  from the simulations. Near the tip of a main branch, most of the sidebranches born are still prominent, making it difficult in deciding which ones are winning the competition for growth; near the centre of the cluster growth is inhibited by screening from the other main branches. A possible measure of  $\lambda$  would be to consider only those branches that cross the equivalent solid wedge of head angle  $\theta_{\text{eff}}$ . We tried to analyse the spacing along the main branches in fig. 1 using this method, and found values for  $\lambda(\phi)$  that fluctuate strongly, but which are not inconsistent with our prediction. At least, the simulations seem to show the spacing  $\lambda$  increasing with decreasing  $\phi$ , in agreement with the trend of the analytical results. For comparison, the insets of fig. 1 are constructions of the predicted asymptotic structures, using the theoretical values of table I.

To conclude, we have presented a theory for the growth of a dendrite in which the spacing of the sidebranches and the head angle at the tip of the dendrite are solely determined by the anisotropy. We have found a self-consistent correction to the wedge

TABLE I. - Theoretical results for  $\lambda$  and  $\theta_G$  for various anisotropies  $\phi$ . The value of  $\theta_G$  that corresponds to the envelope that encloses the tips of the sidebranches in the simulations, is included for comparison. Note that the work of ref. [11] shows that sixfold growth is unstable with respect to loss of major fingers, so that its angles are less clearly defined.

Sidebranch angles	Theoretical values			Simulation measured from ref. [5]
	$\lambda$	$\theta_{\text{eff}}$	$\theta_G$	$\theta_G$
$\frac{2\pi}{3}$	0.834	174.5°	172.6°	(172 ± 1)°
$\frac{2\pi}{4}$	0.653	168.8°	164.0°	(164 ± 1)°
$\frac{2\pi}{5}$	0.524	165.9°	158.5°	(162 ± 2)°
$\frac{2\pi}{6}$	0.437	165.2°	155.8°	(150 ± 5)°

approximation. As mentioned above, the coupling between sidebranches on either side of the main stem is expected to be very weak. Analysis of the coupling between the two terms in  $g(z)$  eq. (2) leads to a stronger instability when the sidebranches on the upper side are *symmetric* with those on the lower than in the antisymmetric configuration. Although one may therefore expect the symmetric mode to be selected, the simulations show no such correlation. This may be due to the coupling being too weak to survive the destroying effect of small random structural fluctuations (noise), present in these DLA structures.

\* \* \*

We would like to thank P. MEAKIN for supplying and allowing us to reproduce fig. 1. This research was supported in part by Unilever and the United Kingdom Science and Engineering Research Council.

## REFERENCES

- [1] See, e.g., VICSEK T., *Fractal Growth Phenomena* (World Scientific, Singapore) 1989.
- [2] WITTEN T. A. and SANDER L. M., *Phys. Rev. Lett.*, 47 (1981) 1400.
- [3] TANG C., *Phys. Rev. A*, 31 (1985) 1977; KERTESZ J. and VICSEK T., *J. Phys. A*, 19 (1986) L-257.
- [4] NITTMANN J. and STANLEY H. E., *Nature (London)*, 321 (1986) 603.
- [5] ECKMANN J., MEAKIN P., PROCACCIA I. and ZEITAK R., *Phys. Rev. A*, 39 (1989) 3185.
- [6] BALL R. C., BRADY R. M., ROSSI G. and THOMPSON B. R., *Phys. Rev. Lett.*, 55 (1985) 1040.
- [7] TURKEVICH L. A. and SCHER H., *Phys. Rev. Lett.*, 55 (1985) 1026.
- [8] A hierarchical construction in this spirit was introduced by HALSEY T. C., *Europhys. Lett.*, 4 (1987) 315.
- [9] The idea of marginal stability has been introduced in a different context by LANGER J. S., *Rev. Mod. Phys.*, 52 (1980) 1.
- [10] MULLINS W. W. and SEKERKA R. F., *J. Appl. Phys.*, 34 (1963) 323.
- [11] BALL R. C., *Physica A*, 140 (1986) 62.
- [12] NIEMEYER L., PIETRONERO L. and WEISMANN H. J., *Phys. Rev. Lett.*, 52 (1984) 1033.
- [13] For a general review of conformal transformations, see, e.g. MORSE P. M. and FESHBACH H., *Methods of theoretical physics*, Part. 1, Ch. 4 (1953) p. 445.